DESIGN OF A SPHERICAL CAM MECHANISM FOR AN AUTOMOTIVE DIFFERENTIAL

Mayank Chaudhary, Jorge Angeles, Alexei Morozov
Department of Mechanical Engineering, McGill University, Montréal, Canada.
Email: mayank91@cim.mcgill.ca; jorge.angeles@mcgill.ca; alexvit@cim.mcgill.ca

ABSTRACT

Spherical cam-follower mechanisms are attractive alternatives to bevel gears, as they provide low backlash and low friction losses. The design of such a mechanism is reported here, to be incorporated in an automotive differential, whose bevel pinions and side gears are substituted by spherical cams and roller-carriers, respectively. Critical to the design of cam mechanisms is the generation of the cam-profile, free of undercutting. The profile, generated using computer algebra, is analyzed for singularities, including cusps and double points. The pressure angle, an important factor that governs the effective force transmission of cam mechanisms, is duly kept within acceptable limits. Conclusions are drawn on the suitability of cam mechanism developed for automotive applications.

Keywords: two-degrees-of-freedom spherical cam mechanism; cam-profile generation; pressure angle.

CONCEPTION D'UN MÉCANISME A CAMES SPHÉRIQUES POU UN DIFFÉRENTIEL AUTOMOBILE

RÉSUMÉ

Les mécanismes sphériques à cames sont des alternatives avantageuses par rapport aux engrenages coniques, puisqu'ils offrent un jeu plus limité que ces derniers et de faibles pertes par frottement. Cette communication porte sur la conception d'un mécanisme de ce type, qui est destiné à fonctionner comme différentiel automobile, dans lequel les engrenages satellites et planétaires sont remplacés par des cames sphériques et de porte-roulements coniques. La production du contour de la came, qui joue un rôle essentiel dans la conception de cette dernière, doit être libre de toute contre-dépouille. En outre, l'analyse du contour généré par le calcul formel permet de s'assurer que le contour est libre de singularités, soit de pointes et des points doubles. L'angle de pression, qui joue un rôle primordial dans la transmission de la force, est maintenu dans des limites acceptables. La communication conclut par une recommandation sur la pertinence des mécanismes à cames dans les applications automobiles.

Mots-clés : mécanisme de came sphérique à deux degrés de liberté ; génération du contourl de la came sphérique ; angle de pression.

NOMENCLATURE

M	Number of lobes of spherical cams
N	Number of conical rollers on the roller-carrier
$\mathbf{f}$	Unit vector along the force applied by the cam
$\bar{\mathbf{f}}$	Unit vector parallel to the force applied by the roller-carrier
$\mathbf{v}_c$	Velocity vector of the cam at the intersection of the generatrix of the cam conical surface with the unit sphere.
$\mathbf{v}_r$	Velocity vector of the roller-carrier at the intersection of roller axis and unit sphere.
$\mathbf{Q}_i(\cdot)$	Matrix representing a rotation about the i-axis through angle $(\cdot)$
Greek symbols	
ϕ	Angle of rotation of the roller carrier
ψ	Angle of rotation of the cam
μ_p	Pressure angle under positive action
μ_n	Pressure angle under negative action
α_3	Angle of the roller carrier

1. INTRODUCTION

Spherical cam mechanisms appear as feasible replacements for bevel gears. Cam mechanisms offer attractive alternatives in terms of torque transfer, stiffness, with lower backlash and lower friction at the coupling between two intersecting shafts. An innovative design of a pitch-roll wrist using spherical cam-roller pairs instead of bevel gears was proposed recently [1]. However, there are some disadvantages inherent to cam mechanisms such as higher manufacturing cost and a variable pressure angle. For this reason, the applications of cam mechanisms need to be investigated while keeping in mind the trade-off between their advantages and disadvantages. In the paper the design of a spherical cam mechanism developed for an automotive differential is proposed.

The synthesis methodology of the spherical cam profile is first discussed, the critical design parameters leading to singularities and subsequent undercutting are identified. The pressure angle is one of the most important factors that determines the transmission quality of spherical cam mechanisms. Its definition and role in deciding the design-parameter values are explained.

2. CAM-PROFILE SYNTHESIS

The spherical cam mechanism discussed by Bai and Angeles [2] consists of two coaxial conjugate multi-lobe cams (MLC) and two roller-carriers (RC), each with two sets of rollers, one internal, one external, as shown in Fig. 1. The cam profile is generated upon plotting the locus of the contact point of the roller and the cam. First, a coordinate frame is defined with origin at the centre of the unit sphere. Next, a relation between the angular velocities $\dot{\psi}$ of the cam and $\dot{\phi}$ of the roller-carrier is formulated, with $\dot{\psi}$ as the input, $\dot{\phi}$ as the output. Under the assumption that the Z-axis passes through the cam axis of rotation, the other axes and unit vectors are defined relative to the Z-axis .

2.1. Nomenclature

All the elements of a spherical cam mechanism are shown in Fig. 1, with their representative arcs. The Aronhold–Kennedy theorem [2] is used to define the instant axes of rotation of the follower with respect to the cam. The various axes involved in the mechanism, along with their unit vectors, are defined below:

1. $\mathscr{C}$ ($\mathbf{e_p}$): Axis of the roller
2. $\mathscr{D}$ ($\mathbf{e_c}$): Instant axis of rotation of the roller with respect to the cam

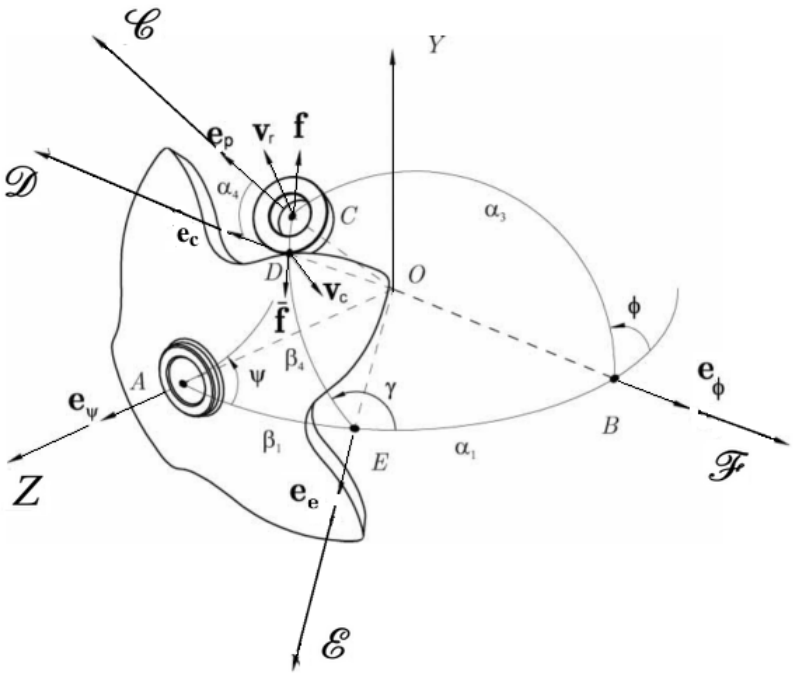

Fig. 1. Axes and angles defined for the spherical cam mechanism

3. $\mathscr{E}$ ($\mathbf{e}_e$): Instant axis of rotation of the cam with respect to the follower
4. $\mathscr{F}$ ($\mathbf{e}_\phi$): Axis of rotation of the follower shaft, to which the roller axis is rigidly attached
5. Z ($\mathbf{e}_\psi$): Axis of rotation of the cam

Unit vectors are defined in Fig. 1, parallel to the foregoing axes. The various angles in Fig. 1 define the relations between the various axes :

1. α_1: Angle between the axis of the cam and that of the roller-carrier, $\angle AOB$
2. α_3: Angle subtended at the centre of sphere by the arc of the roller-carrier, $\angle BOC$
3. α_4: Angle between $\mathscr{C}$ and $\mathscr{F}$, $\angle COD$
4. β_1: Angle between the cam axis and the instant axis of rotation of the follower with respect to the cam, $\angle AOE$
5. β_4: Angle between the axis of the roller and the instant axis of rotation of the follower with respect to the cam, $\angle COE$

2.2. Cam-Profile Generation Procedure

For a spherical cam mechanism with M lobes and N rollers in the roller carrier, the angular velocity of cam and roller-carrier are defined as $\dot{\psi}$ and $\dot{\phi}$, respectively. With $\phi_0 = (1-1/N)\pi$ [2], we have

$$\phi = -\frac{M}{N}\psi + \phi_0, \quad \tan\beta_1 = \frac{\phi' \sin\alpha_1}{\phi' \cos\alpha_1 - 1} \tag{1}$$

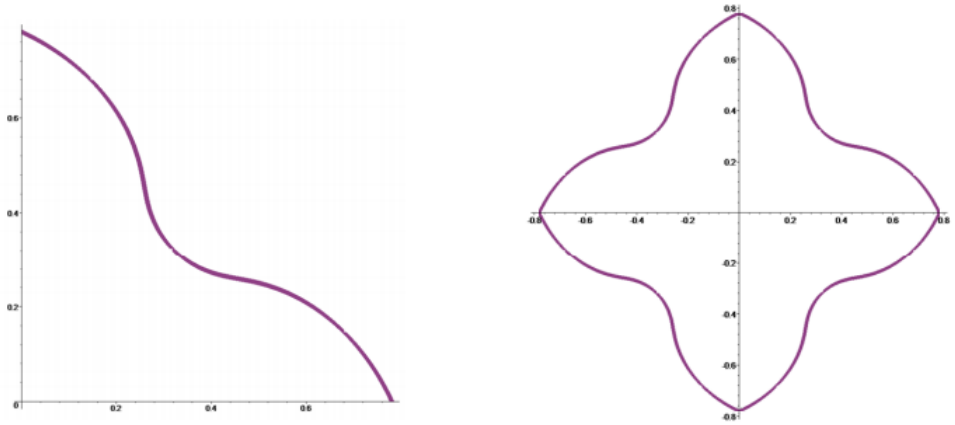

Fig. 2. (a) Two-dimensional plot of one period of the cam profile; (b) The complete two-dimensional plot of the cam profile with its four lobes

Using the definition of the vectors along the axes of rotation and the angles subtended on the unit sphere along with the orthogonal matrices representing rotations, the relations below follow:

1. $\mathbf{e}_\psi = \mathbf{e_z} = [0 \quad 0 \quad 1]^T$
2. $\mathbf{e_p} = \mathbf{Q_y}(\alpha_1)\mathbf{Q_z}(\phi)\mathbf{Q_y}(\alpha_3)\mathbf{e_z}$
3. $\mathbf{e_e} = \mathbf{Q_y}(\beta_1)\mathbf{e_z}$
4. $\mathbf{e}_\phi = \mathbf{Q_y}(\alpha_1)\mathbf{e_z}$

The unknown quantities are calculated using the relations

$$\beta_3 = \beta_4 - \alpha_4, \quad \cos\beta_4 = \mathbf{e}_e{}^{\mathrm{T}}\mathbf{e}_p \tag{2}$$

$$\cos\gamma = \csc(\alpha_1 - \beta_1)\csc\beta_4[\cos\alpha_3 - \cos(\alpha_1 - \beta_1)\cos\beta_4] \tag{3}$$

The position vector for the cam-profile generation is obtained by means of vector $\mathbf{e}_c$ and the proper orthogonal matrix representing the rotation about the cam-axis through the angle ψ of cam rotation, namely,

$$\mathbf{s}_c = \mathbf{Q}_z^{\mathrm{T}}(\psi)\mathbf{e}_c = \begin{bmatrix} \cos\psi\sin\gamma\sin\beta_3 - \sin\psi(\cos\beta_1\cos\gamma\sin\beta_3 + \sin\beta_1\cos\beta_3 \\ -\sin\psi\sin\gamma\sin\beta_3 - \cos\psi(\cos\beta_1\cos\gamma\sin\beta_3 + \sin\beta_1\cos\beta_3 \\ -\sin\beta_1\cos\gamma\sin\beta_3 + \cos\beta_1\cos\beta_3 \end{bmatrix} \tag{4}$$

The two-dimensional plot obtained by varying the $x-$ and $y-$ coordinates, both functions of the input angle ψ, for values of ψ varying from $\psi_{\min}$ to $\psi_{\max}$, is shown in Fig. 2(a). The plot is confined to the first quadrant. The complete two-dimensional cam profile is obtained by rotating the foregoing plot $M-1$ times where M is the number of lobes, defined as 4 in our case, as shown in Fig. 2(b).

In fact, eq. (4) does not produce the whole profile for a full turn of the cam, $0 \leq \psi \leq 2\pi$, but only for $1/M$ of a turn; even this fraction of a turn is incomplete. In order to obtain the full 1/4 of a turn in our case, an

extension angle σ was introduced. This was done upon zeroing the second component, $(\mathbf{s}_c)_2$, of vector $\mathbf{s}_c$ of eq. (4):

$$(\mathbf{s}_c)_2|_{\psi=\sigma} = 0 \tag{5}$$

With this value, the range of motion of the cam, $[\psi_{min}, \psi_{max}]$, was obtained as

$$\psi_{min} = -\sigma - \frac{2\pi}{M}, \quad \psi_{max} = \sigma \tag{6}$$

The spherical curve representing the cam-profile is shown in Fig. 3, obtained as the intersection of the conical surface of the cam with the sphere on which the spherical mechanism is based.

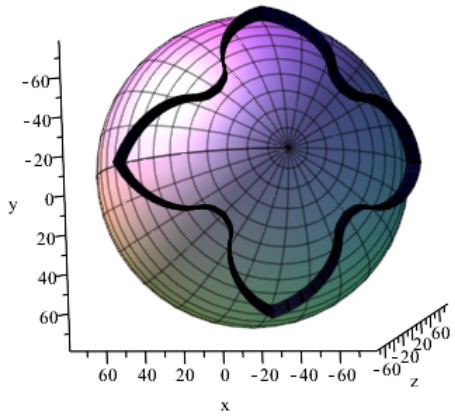

Fig. 3. Conic surface defining the spherical cam-profile intersecting the sphere on which the spherical mechanism is based

3. PRESSURE ANGLE

The pressure-angle is defined as that between the line of action of the force applied by the driver element and the direction of the velocity of the contact point on the driven element. A variable pressure angle is a major detriment when replacing bevel gears with cam mechanisms, as gears offer a constant pressure angle. The maximum value of the pressure angle must be kept within an acceptable range to substitute bevel gears with a spherical cam mechanism. The mechanism considered in this paper is reversible, which means that both the cam and the roller-carrier can play the role of the driver, the other of the driven element. When the cam drives the roller-carrier, the mechanism is said to operate under positive action. The pressure angle under positive action, denoted by μ_p, is given as

$$\tan\mu_p = \frac{\| \mathbf{f} \times \mathbf{v}_r \|}{\mathbf{f} \cdot \mathbf{v}_r} \tag{7}$$

Here $\mathbf{f} = \mathbf{e}_p \times (\mathbf{e}_p \times \mathbf{e}_e)$ and $\mathbf{v}_r = \mathbf{e}_p \times \mathbf{e}_\phi$. In case of negative action the roller-carrier drives the cam, the pressure angle then being denoted by μ_n, namely,

$$\tan\mu_n = \frac{\| \bar{\mathbf{f}} \times \mathbf{v}_c \|}{\bar{\mathbf{f}} \cdot \mathbf{v}_c} \tag{8}$$

where $\bar{\mathbf{f}} = \mathbf{e}_c \times (\mathbf{e}_e \times \mathbf{e}_c)$ and $\mathbf{v}_c = \mathbf{e}_\phi \times \mathbf{e}_c$.

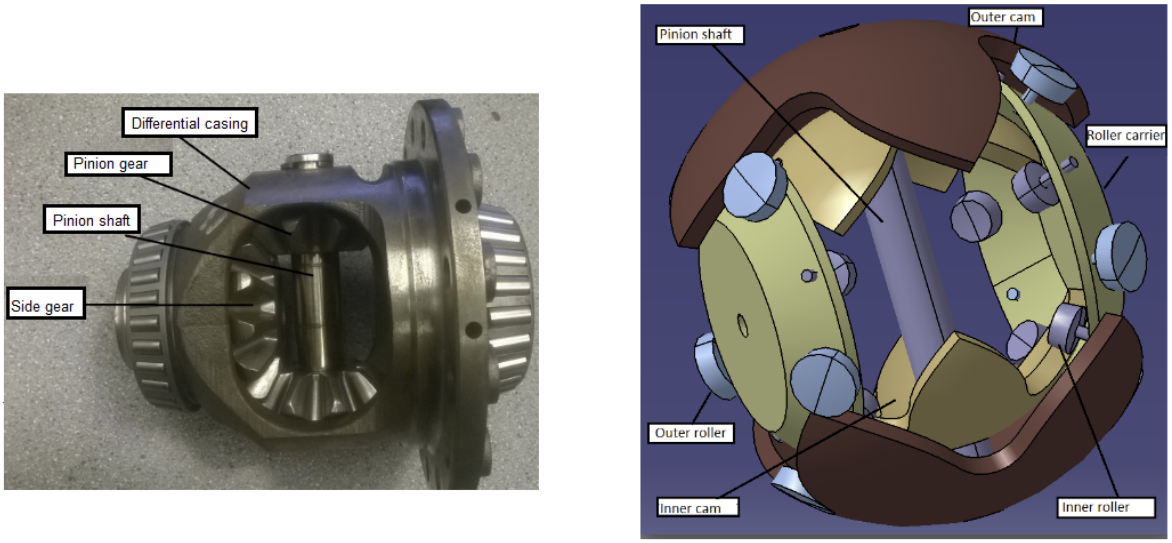

Fig. 4. (a) Differential mechanism; (b) Spherical cam-roller mechanism to function as an automotive differential

4. APPLICATION: AUTOMOTIVE DIFFERENTIAL

Automotive transmissions based on cam have only recently appeared in the industry. The design of infinitely variable transmission with spherical cams was proposed [3], [4]. Other applications of cam mechanisms in automotive design have been reported, but these are limited to the gearbox transmission [7], [8]. Nevertheless, other possible technical solutions are not available in the automotive industry. In this paper, the spherical cam mechanism is considered as applied to an automotive differential, which is usually based on epicyclic (planetary) gear trains. A planetary gear train based on cams was proposed recently by Hsieh [5]. The design of an automotive differential along the same lines is proposed in this paper. The final-drive differential carrier assembly in a four-wheeled vehicle provides means for allowing one traction wheel to travel faster than the other when the vehicle negotiates a corner. As can be seen in Fig. 4(a) the differential carrier subassembly consists of: four bevel gears and one pinion shaft. Two bevel gears, the differential side gears, are splined to the axle shafts (the left-hand axle shaft is splined to the output shaft, which connects output shaft with side gear). The two outer bevel gears i.e., the pinion gears, act as idlers to transfer the power from the differential carrier to the differential side gears. The differential pinion gears also balance the power load between the differential side gears while allowing unequal axle angular speeds when the vehicle negotiates a corner under these conditions, the outside wheel turning faster than its inside counterpart, and the differential pinion gears spinning with respect to the crown gear as they turn around the differential side gears. This allows the speed of the crown gear to be delivered unevenly to the two wheels.

4.1. Spherical Cam-roller Mechanism as Automotive Differential

The proposed automotive-differential model incorporating spherical cam-roller mechanism is shown in Fig. 4(b). Two sets of co-axial conjugate cams are used with corresponding sets of rollers mounted on two opposite sides of the roller-carrier. As each roller comes into contact with one cam, a single cam mechanism is formed; as contact is lost from one follower side, a roller from the other side begins to engage the conjugate cam, thus generating positive action throughout the whole cycle.

Each roller along with its roller-carrier plays the role of a differential side gear. Each pair of co-axial

conjugate cams plays the role of a differential pinion gear. When the vehicle is driven along a straight line, the set of cams and roller-carrier rotate as a single unit.

When the vehicle turns a corner, the roller-carrier turns around the set of cams. The inner rollers and outer rollers are coupled with the inner cam and the outer cam via a higher kinematic pair. The inner cam has a fixed orientation with respect to its corresponding outer cam, the two sets of co-axial conjugate cams being freely mounted on the pinion shaft.

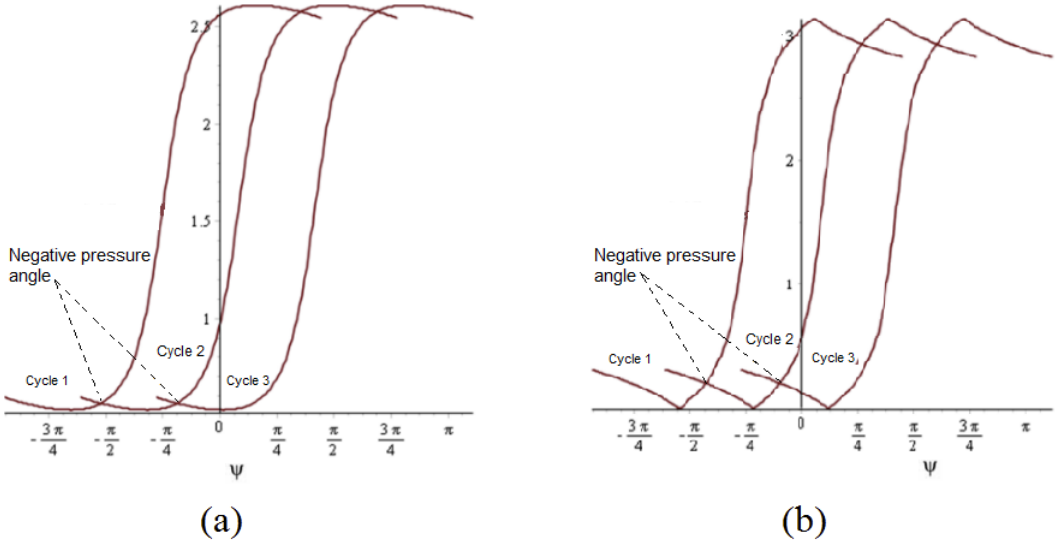

Fig. 5. (a) Pressure-angle for $M = 4$ and $N = 5$, (b) Pressure-angle for $M = 4$ and $N = 4$

4.2. Pressure Angle

A parametric expression for the pressure-angle is generated with the parameter ψ using eq. (8), plotted by varying ψ from 0 to $-2\pi/M$ and for different values of M and N. A plot of the pressure angle for $M = 4$ and $N = 5$, for three cycles, is shown in Fig. 5(a). The minimum operating pressure angle is the minimum of the plot, the maximum operating pressure angle being the value at the intersection of the pressure-angle plot of cycle 1 with the pressure-angle plot of cycle 2, as shown in Fig. 5(a).

A special case arises when the number of lobes equals the number of rollers i.e. $M = N$, in which case the minimum operating pressure angle takes the value of 0 rad, as shown in Fig. 5(b). This particular combination of numbers of lobes and rollers is unfeasible, as the radial component of the normal force becomes zero, the contact force between cam and follower thereby vanishing.

Similarly, pressure-angle plots are obtained for $M = 3$ and $M = 4$ with $N = 3,4,5,6,7,8$. The minimum and maximum operating pressure-angle values are observed from the plot and displayed in Table 1. It can be observed that, for a fixed value of M, the pressure angle varies linearly with N. With the aim to keep the pressure angle low, the two feasible combinations are, $\{M = 3, N = 4\}$ and $\{M = 4, N = 5\}$.

4.3. Final-Drive Ratio

The final-drive ratio is defined as the ratio of the drive-shaft pinion gear to the sun gear bolted to the differential casing. The final-drive assembly is a planetary gear set consisting of: a final-drive sun gear splined to the final-drive sun gear shaft; a final-drive planetary pinion; two pinion and side gears located in the differential and the final-drive carrier assembly, as shown in Fig. 6.

The final-drive planetary gear set operates as a speed reducer all the time. Power through the final-drive

Number of lobes, M	Number of rollers, N	Minimum operating pressure-angle (rad)	Maximum operating pressure-angle (rad)
3	3	0	0.21
	4	0.63	0.66
	5	0.88	0.9
	6	1.02	1.11
	7	1.1	1.11
4	4	0	16.62
	5	0.52	0.57
	6	0.78	0.8
	7	1.01	1.02
	8	1.02	1.03

Table 1. Pressure-angle range for varying number of lobes and rollers

sun gear shaft drives the final-drive sun gear in the same direction as the engine rotation, but forces the final-drive planetary pinion gears to rotate in the opposite direction inside the final-drive internal gear. Since the latter is held stationary by the case, the differential and the final-drive carrier assembly rotate in the same direction as the engine. The gear ratio of the final-drive and differential assemblies perform the same functions as the ring and pinion gears in a conventional rear axle unit. A fixed final-drive axle ratio is required to match the engine power and drive train to the vehicle requirements for all normal operating conditions. As a reference, the differential mechanism of the GM 4T65-E Hydramatic Transmission system [6] was

Number of lobes, M	Number of rollers, N	Differential ratio	Final-drive ratios				
3	3	1	3.05	3.29	3.73	4.1	4.56
	4	0.75	2.28	2.46	2.79	3.07	3.42
	5	0.6	1.83	1.97	2.23	2.46	2.73
	6	0.5	1.52	1.64	1.86	2.05	2.28
	7	0.42	1.3	1.41	1.59	1.75	1.95
4	4	1	3.05	3.29	3.73	4.1	4.56
	5	0.8	2.44	2.63	2.98	3.28	3.64
	6	0.66	2.03	2.19	2.48	2.73	3.04
	7	0.57	1.74	1.88	2.13	2.34	2.6
	8	0.5	1.52	1.64	1.86	2.05	2.28

Table 2. Final-drive ratios for varying number of lobes and rollers

considered. The final-drive ratios for medium duty trucks, as per the GM 4T65-E transmission, available commercially are 3.05, 3.29, 3.73, 4.1, and 4.56. These ratios exist when the gear ratio between the differential planet and the differential side gear, called the differential ratio, is 1:1. If the differential ratio is varied, the final-drive ratio is multiplied by the new differential ratio. An important factor to consider while fixing the new differential ratio is to obtain the new final-drive ratio to be one of the standard ratios available or close to it. For the cam-roller mechanism, where the role of the differential pinion is played by a set

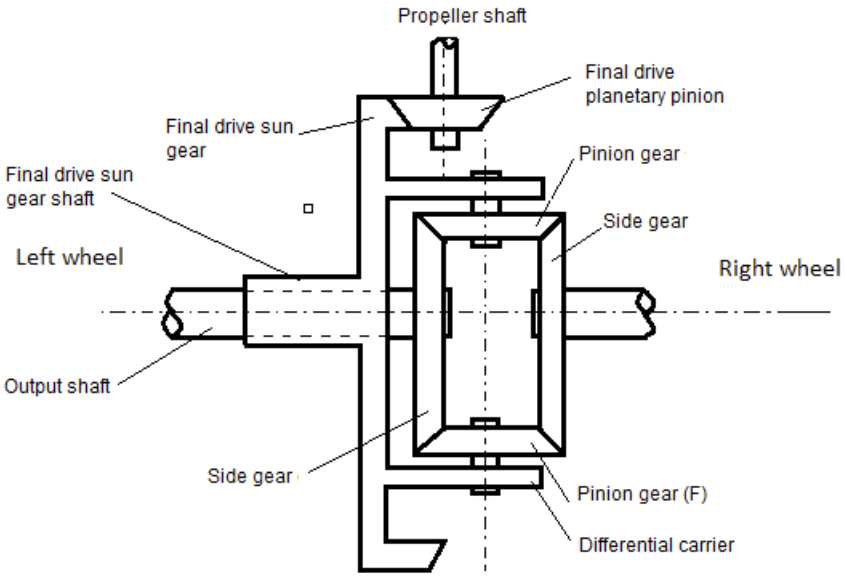

Fig. 6. Schematic of an automotive differential

of co-axial conjugate cams and the role of the differential side gears is played by rollers and their carrier, the differential ratio d_r is defined as M/N. The final-drive ratios are obtained for $M = 3$ and $M = 4$, with $N = 3, 4, 5, 6, 7, 8$ as shown in Table 2.

4.4. Inference

As can be observed from Table 2, with the various differential ratios, the combinations $\{M = 3, N = 4\}$ and $\{M = 4, N = 5\}$ lead to final-drive ratios of 3.07 and 3.28, respectively. The former final-drive ratio is off by 0.02 from the standard value of 3.05, with the latter being off by 0.01 from the standard value of 3.29. Moreover, the combination $\{M = 4, N = 5\}$ leads to a lower value of operating pressure-angle, as compared with the combination $\{M = 3, N = 4\}$. Thus, for the minimum and the maximum operating pressure-angle range, and optimum final-drive ratio, the values below are assigned:

- Number of lobes (M): 4
- Number of rollers (N): 5

These values lead to:

- Final-drive ratio: 4.1
- Minimum operating pressure angle: 0.52 rad
- Maximum operating pressure angle: 0.57 rad

5. CONCLUSIONS

The spherical cam mechanism was discussed as a possible substitute for the bevel gear automotive differential. The cam mechanism was designed as a replacement of a differential, using the GM 4T65-E transmission system as a reference to assign the various parameter values. Two important parameters were

discussed, pressure-angle and final-drive ratio, to decide the number of lobes and the number of rollers for the spherical cam-roller mechanism. For design purposes, a comparative study was conducted via the finite element analysis (FEA) of the two mechanisms under consideration, the results to be reported in a forthcoming paper. The maximum von Mises stress was found in individual components for comparison. The spherical cam-roller mechanism proves to be a viable, and potentially beneficial, substitute for an automotive bevel-gear differential when analyzing equivalent stress distributions. A preliminary analysis showed that the volume of the cam-based differential can be reduced by about 27% in comparison with a conventional one with similar ratio and power capacity. The performance of the cam-roller differential regarding noise, backlash and durability should be tested and compared with the performance of current differentials. Further work continues on cam design and FEA to achieve higher transmission quality and smoothness of cam profiles.

6. ACKNOWLEDGMENT

The research work reported here was supported by a grant from Automotive Partnerships Canada, APCPJ418901-11.

REFERENCES

1. C. P. Teng, S. Bai, J. Angeles, 2007, Shape Synthesis in Mechanical Design, Acta Polytechnica Vol. 47, No. 6.
2. Bai, S.and Angeles, J., 2009, The design of spherical multilobe-cam mechanisms, *Journal of Mechanical Engineering Science*, Vol. 223, No. 3, pp. 473–482.
3. D.Lahr, Patent US8425364 Cam-based infinitely variable transmission, Apr. 23, 2013.
4. D.F. Lahr, D.W. Hong, 2006, The Operation and Kinematic Analysis of a Novel Cam-based Infinitely Variable Transmission, Proceedings of IDETC /CIE2006 ASME2006 International Design Engineering Technical Conferences Computers and Information in Engineering Conference, September 10-13.
5. W.-H. Hsieh, 2013, Kinetostatic and mechanical efficiency studies on cam-controlled planetary gear trains (Part I)–Theoretical analysis, Indian Journal of Engineering Materials Sciences Vol. 20, pp. 191–198.
6. Power Train Group General Motors Corporation, 1997, *GM Hydramatic 4T65-E Transmission Manual*.
7. K.P. Patil, K.M. Jagadale, B.S. Patil , M. Prashant, 2013, Cam Based IVT, IOSR Journal of Mechanical and Civil Engineering, Special Issue: Proceedings of Second International Conference on Emerging Trends in Engineering 2013, Mechanical Group, Vol. 3, pp. 13–20.
8. M.A. Amjad, 2010, A Novel Cam-Based Infinitly Variable Transmission, Journal of Kerbala University, Vol. 8, No. 4, pp. 61–74.